Preparation and Photocatalytic activities of Fe^{3+} Doped Nanometer TiO_2 Composites

Xiaohong Hu, Taicheng An*, Maolin Zhang, Guoying Sheng and Jiamo Fu

State Key Laboratory of Organic Geochemistry, Guangdong Key Laboratory of Environmental Resources Utilization and Protection, Guangzhou Institute of Geochemistry, Chinese Academy of Sciences, Guangzhou 510640, CHINA

*antc99@gig.ac.cn

Abstract

Nanometer Fe^{3+} doped TiO_2 and TiO_2/Fe_2O_3 coupled oxides photocatalysts were prepared with different content ferric citrate and different opposite anions of iron using the $Ti(SO_4)_2$ precipitation method. The precursors of nanometer TiO_2 were analyzed by thermogravimetric and differential thermal analyses (TG/DTA) and both nanometer photocatalysts were characterized by X-ray diffraction (XRD), transmission electron microscope (TEM) and UV–VIS diffuse reflectance spectrum (DRS). The results showed that the mean size of nanometer TiO_2 in both photocatalysts decreased with the increase in Fe^{3+} doped content. The photocatalytic activities of prepared catalysts were evaluated under UV light irradiation using methyl orange as a mode organic pollutant in water. The results showed that a small amount of iron dopants in TiO_2 crystalline matrix could enhance the photocatalytic efficiency. The prepared TiO_2 samples exhibited even higher photocatalytic activities than that of Degussa P25, the optimal amount of doped Fe^{3+} was 0.05%. However, with increase of iron element amount, at 25% and 50% contents, the nanometer particle becomes the coupled oxides of TiO_2/Fe_2O_3. Moreover, the effect of different doped anions coming from different ferrous salts on the photocatalytic activities of Fe^{3+}/TiO_2 was also investigated, and the best doped opposite anion is found as SO_4^{2-}.

Key words: Photocatalyst, TiO_2, Iron doped, Coupled oxides, Methyl orange and Degradation.

Introduction

Photocatalysis utilizing semiconductor materials as a photocatalyst has attracted extensive attentions of the academic communities in recent decades. Upto know, titanium dioxide in the anatase form, which has the advantages of being non-toxic, insoluble and comparatively inexpensive, is the most commonly used photocatalyst because of its reasonable photoactivity[1]. Thus TiO_2 photocatalytic oxidation of organic pollutants has been one of the most active fields in terms of environmental pollution control because organic pollutants can be easily degraded into CO_2 and H_2O by this advanced oxidation technology[2-3]. A major challenge in heterogeneous photocatalysis is how to increase charge separation efficiency of photocatalyst and then to improve the photocatalytic efficiency by some surface modification means[4-7]. Many transitional metal ion dopants have been extensively investigated for the TiO_2 system[4, 8-9]. In fact, the photocatalytic activities of the doped TiO_2 virtually depend on the foreign metal ion species, nature and concentration, besides the preparation methods, the thermal treatments[10-11]. Recently, special efforts have been dedicated to doping TiO_2 with Fe^{3+}.[9,12,13] Among various transition metals, Fe^{3+} ion is chosen mainly because the Fe^{3+} radii (0.69 Å) is very near the Ti^{4+} radii (0.745 Å), so Fe^{3+} will substitute Ti^{4+} easily into the lattices of TiO_2 [5]. Fe^{2+}/Fe^{3+} energy level lies close to Ti^{3+}/Ti^{4+} level. Fe^{3+} can provide a shallow trap for photo-generated hole and electron in anatase, illuminating Fe^{3+} can enhance the photogenerated electron-hole pair separation and quantum yield[5, 13]. Moreover, the effect of different accessorily added anions on the photocatalytic activity of doped TiO_2 when the ferric ions were doped with different ferric salt has not been investigated so far.

In the present paper, nanometer Fe^{3+} doped TiO_2 and TiO_2/Fe_2O_3 coupled oxides photocatalysts were prepared by a simple synthetic route based on the precipitation of $Ti(SO_4)_2$ from the point of views of practical use and commerce, especially the precursor of TiO_2 was dried over steam bath at 80°C with ultrasonic wave promoting iron ions and surfactants uniformly distributed in the surfaces of precursors of TiO_2, preventing particles agglomeration. The photocatalytic degradation activities of the prepared nanometer Fe^{3+} doped TiO_2 and TiO_2/Fe_2O_3 coupled oxides photocatalysts were examined using methyl orange (MO) as a model organic compound.

Material and Methods

The reagents ($FeC_6O_7.4H_2O$, $FeCl_3$, $Fe_2(SO_4)_3$, $Fe(NO_3)_3$, $Ti(SO_4)_2$, $NH_3.H_2O$, MO) are all analytic reagent grade. The photocatalytic reactions take place in a 100 ml Pyrex glass bottle, under illumination by a 150W high pressure Hg lamp (GGZ150, Shanghai Yaming Lighting Co.

Ltd.) with a maximum emission at about 365 nm. The MO concentration at the intervals was analyzed by 722S spectrophotometer (Shanghai Precision & Scientific Instrument Co. Ltd.) at its maximum absorption wavelength of 464 nm. The thermal stability of the titanium hydroxide was studied by TG/DTA (Netzsch TG209). A Rigaka D/max-1200 diffractmeter was used to determine the crystal phase composition of the titanium dioxides and TiO_2/Fe_2O_3 coupled oxides. And a transmission electron microscope (LEO 1530 VP TEM) was used to observe the shape and size of the prepared photocatalysts. A Hitachi UV-3010 UV-vis spectrophotometer was used to carry out the UV-Vis diffuse reflectance spectroscopy and the $BaSO_4$ high reflectance white optical paint was used as a reference material.

Preparation of nanometer Fe^{3+} doping TiO_2 and TiO_2/Fe_2O_3 coupled oxides: The precursor of nanometer TiO_2 was prepared using the precipitation method. $Ti(SO_4)_2$ was used as the starting material and $NH_3.H_2O$ used as the precipitant. $Ti(SO_4)_2$ were dissolved in 200 ml of distilled water (0.1M), the 1:1 (v/v) diluted NH_3 aqueous solution was added dropwise and white slurry was formed substantially. The resulting slurry was continuously stirred for 2 h, filtered and washed with distilled water until the sulphate ions were removed (as confirmed by the $BaCl_2$ test), then the ethanol and surfactants (Sorbitan fatty acid ester, Span 80; Polysorbate, Tween 20) were added into to get the slurry again. The slurry was stirred for 0.5 h further and subsequently dried over steam bath at 80°C with ultrasonic (QK-3200E, 150w Ultrasonic Instrument Co., Jiangsu, China) to obtain the precursor of TiO_2. Then the precursor was calcined at 450 °C for two hours to form the anatase crystal phase of TiO_2.

As Fe^{3+} doping TiO_2 and coupled oxides concerned, a certain amount of dissolved ferric citrate (FC) was doped into the foregoing washed white slurry according to different mole ratios of Fe^{3+}:TiO_2 with 0%, 0.01%, 0.05%, 0.1%, 0.5%, 1%, 25%, 50%, As for different ferric anion salt was doped, 0.05% of mole ratio for different iron salt, such as $FeCl_3$, $Fe_2(SO_4)_3$, $Fe(NO_3)_3$ and FC were added for comparison. And the resulted slurry was also treated with the same procedures previously described.

Photocatalytic reactor and procedure: The photocatalytic reaction was carried out in a home-made Pyrex glass reactor where a UV high pressure mercury lamp with quartz protecting tube was placed in the center of the reactor (see Fig.1). The cooling water flows into the annulus surrounding the reactor in order to maintain a constant temperature during the experiment. Prior to irradiation, 100 ml of 40 mg/l MO solution was added together with 0.2 g prepared photocatalysts, the suspension was stirred in dark for 30 min further to establish adsorption equilibrium. Then the photocatalytic reaction was started when the suspension containing photocatalyst were irradiated under the UV light.

At given time intervals, 3 ml suspension was taken from the reactor and centrifuged at 9000 rpm for 10 min and filtered through a 0.22 ìm millipore filter. Then, the filtrate was analyzed by spectrophotometer at its maximum absorption wavelength (ca. 464 nm). The degradation efficiency of the MO can be calculated according to the formula listed as follows:

$$\text{Degradation efficiency} = (1-C_t/C_0)*100\%,$$

where C_0 and C_t represent the initial concentration and the concentrations at reaction time t, respectively.

Some synthesized samples and P25 TiO_2 were also chosen to perform additional photocatalytic experiments at the same time intervals under the sunlight. The reactor used was a Pyrex glass beaker of 1000ml. The average light intensity was about 200 $\mu W/cm^2$, as measured by a UV radiometer (made in the Photoelectric Instrument Factory of Beijing Normal University) with the peak intensity of 365 nm.

Results and Discussion

Thermogravimetric and differential thermal analyses (TG/DTA) of the precursor of TiO_2 : The thermogravimetric and differential thermal analyses (TG/DTA) curves for the precursor of nanometer TiO_2 are shown in Fig. 2. The TG curve indicated the weight loss in three stages with two endothermic peaks at 77.9°C, 134.0°C and an exothermic peak at 268 °C. The total weight loss of around 43.4% is observed between room temperature and 689.1 °C in three stages. The weight loss at 77.9°C was attributed to the loss of ethanol while the weight loss at 134.0 °C was ascribed to the loss of combined water. However, the exothermic peaks from 170°C to 268.6 °C were attributed to the elimination and combustion of surfactants in the precursor of nanometer TiO_2. From 268 °C to 689°C, the hydroxide was continuously converted to anatase phase TiO_2, and the exothermic peak at 793.9°C can be tentatively believed as the conversion temperature of TiO_2 from anatase phase to rutile phase[14, 15]. As a result, the calcining temperature was designed as 450 °C for 2 h to prepare smaller size nanometer TiO_2 particle.

The XRD patterns of Fe^{3+} doping TiO_2 and TiO_2/Fe_2O_3 coupled oxides photocatalyst: Fig. 3 showed X-ray diffraction patterns for TiO_2 doped with different content of FC. Typical profiles of anatase phase TiO_2 were obviously seen from all five curves which have standard peaks existed at 2è=25.34, 37.86, 48.10, 53.92, 55.10, 62.72. The strongest peak at 2 degree 25.32 ± 0.06 is assigned to the (101) lattice plane of TiO_2 (anatase type)[16]. When Fe^{3+} doped content was less than or equal to 1%, any crystalline phase containing iron could not be observed in XRD profiles of Fe^{3+} doped TiO_2. It is possible that Fe^{3+} diffuses into the TiO_2 lattice and substitutes Ti^{4+}. However, with increase of content of FC the typical XRD pattern of Fe_2O_3 at 2è=35.70, 62.90, 30.2

57.48, 43.34 appeared in the XRD profiles of coupled oxides TiO_2/Fe_2O_3 with 25% and 50% FC. The crystallite size of TiO_2 was calculated according to the Scherrer equation[17], and the particles mean sizes are listed in Table 1. From Table 1, it is easily seen that all TiO_2 particles were nanometer scale, moreover the peak is obviously widened when the doping amounts of FC were increased, which implies that the TiO_2 particles crystallite size decreased rapidly. The mean size of TiO_2 was 42.2 nm without Fe^{3+} doped, however, with increase of content of Fe^{3+}, the mean size of TiO_2 becomes smaller and smaller. When the content of Fe^{3+} was up to 25% and 50% in coupled oxides TiO_2/Fe_2O_3, the mean sizes of nanometer TiO_2 particles in coupled oxides were 16.3 and 14.2 nm, respectively. It demonstrates that the addition of iron oxide will restrain the growth of TiO_2 crystallites. This decrease in crystallite size is due to the distribution of added cations at the particles boundary of titania which inhibits particles growth by providing a barrier between the titania particles as reported earlier[18].

Fig. 4 also showed X-ray diffraction patterns of TiO_2 doped with different kind of iron salt but with the same 0.05% Fe^{3+} dopant amount. All samples exhibit only patterns assigned to the well crystalline anatase phase TiO_2. Due to very low Fe^{3+} content, any crystalline phase containing Fe^{3+} also could not be observed by XRD in Fe^{3+} doped TiO_2 because that Fe^{3+} and Ti^{4+} have similar ionic radii (0.79Å versus 0.75 Å). Thus Fe^{3+} may easily substitute Ti^{4+} into TiO_2 lattice. These results support that the current doping procedure with ultrasonic allows uniform distribution of the dopants. When TiO_2 was doped with different kind of ferrous salt with the content of 0.05%, the mean particles size of TiO_2 was almost the same and independent from the kind of ferrous salt (Table 2). The mean sizes of TiO_2 doped with four salts were 21.3, 23.2, 24.3 and 21.6 for FC, $Fe(NO_3)_3$, $FeCl_3$ and $Fe_2(SO_4)_3$ respectively. So as for four added anions, such as SO_4^{2-}, Cl^-, NO_3^- and citrate ions showed little influence on the XRD spectrum of TiO_2.

TEM photographs of Fe^{3+} doping TiO_2 and TiO_2/Fe_2O_3 coupled oxides photocatalyst: Fig.5 and Fig.6 showed the TEM images (with 120,000 magnifications) for prepared TiO_2 with different Fe^{3+} content and with different kind of ferrous salt containing different anions respectively. The morphology of all these particles were of an approximate equable distribution, approximately round or elliptical shapes with particle sizes ranging between 10-50 nm, TEM results showed that the particles had a little aggregated, especially for 25% Fe^{3+}/TiO_2. Moreover, it is obviously seen from the TEM photographs that the mean sizes of TiO_2 particles decreased significantly with increase of the Fe^{3+} content. For example, the mean sizes of pure TiO_2 and 0.05% Fe^{3+}/TiO_2 are about 35.2 and 25.1 nm, respectively, while the mean sizes at the content of 25% in Fe_2O_3/TiO_2 are about 12.5 nm according to XRD spectrum, the sample of TiO_2 containing 50% showed the smallest size of particles. However, from Fig.6, we can easily see that the particle mean sizes with the same content of Fe^{3+} but with different kind anions have few differences. There are some analogous reports[18, 19] that the more ionic dopant ratio increases, the smaller doped TiO_2 particle size is. Thus the TEM observations support the conclusions derived from the XRD data. It can be seen that their values from TEM are smaller than that calculated from XRD. As, this XRD crystal size is based on the supposition that the broadening of the peaks is only due to a size effect but lattice strain was neglected. This may clarify the difference between XRD spectra and TEM observation. Both the TEM photographs and the XRD spectra showed that all the prepared TiO_2 particles were also nanometer scale.

UV–VIS diffuse reflectance spectra of Fe^{3+} doping TiO_2 and TiO_2/Fe_2O_3 coupled photocatalyst: The diffuse reflectance spectroscopy (DRS) was always used to study metal oxides. In a diffuse reflectance spectrum, the ratio of the light scattered from a thick layer of sample and that from an ideal non-absorbing reference sample is measured as a function of the wavelength. The UV-Vis diffuse reflectance spectra of TiO_2 photocatalysts doped with different Fe^{3+} mole ratio and TiO_2/Fe_2O_3 coupled oxides were shown in Fig. 7. From the figure, the wavelengths of the absorption edges in the UV-Vis diffuse reflectance spectra were determined by extrapolating the sharply rising portions and horizontal portions of the UV-Vis curves, defining the absorption edges as the wavelengths at the intersections[21, 22]. From the Fig. 7, it is easily seen that when doping content is at 0.05%, the UV-Vis curves almost overlap with that of pure TiO_2. The presence of the doping ions caused a little absorption increase onset the wavelengths 371 nm and little red shifts at 384 of the absorption edges when compared to the absorption edge of pure TiO_2 at 382.5 nm. Increased absorbance and red shift associated with the present of dopants can be attributed to charge transfer transition between the iron 3d electrons and the TiO_2 conduction or valence band[22]. Especially for the samples with high iron content (>1%), increased absorbance can be ascribed to the d–d transition of Fe^{3+} ($^2T_{2g} \rightarrow {}^2A_{2g}$, $^2T_{1g}$) or the charge transfer transition between interacting iron ions ($Fe^{3+} + Fe^{3+} \rightarrow Fe^{4+} + Fe^{2+}$)[14]. However, the UV–VIS diffuse reflectance spectra doped with the same Fe^{3+} content at 0.05% but containing different kind of anions have not shown any difference in the profiles.

Photocatalytic activity of nanometer iron doped TiO_2 and coupled oxides Fe_2O_3/TiO_2 under UV light and sunlight: To evaluate the photocatalytic activity of the prepared Fe^{3+} doped TiO_2 and coupled oxides Fe_2O_3/TiO_2, and to determine an optimum dosage of Fe^{3+} ion doped in TiO_2, the photocatalytic degradation of MO in aqueous solution was carried out under UV light. From Fig. 8, photocatalytic

efficiency of MO degradation catalyzed by Degussa P25, prepared pure TiO_2 and different Fe/TiO_2 under UV light showed following order: 0.05%Fe/TiO_2 > 0.01%Fe/TiO_2 > 0.1%Fe/TiO_2 > Pure TiO_2 > Degussa P25~ 0.5%Fe/TiO_2 >1%Fe TiO_2. The degradation efficiency increased with increase in the content of Fe^{3+} doped onto TiO_2 up to approximately at 0.05% followed by a decrease in the efficiency with further increase in Fe^{3+} level. It is obvious that less than 0.1% Fe^{3+} is more active than without doped TiO_2, and 0.05% Fe^{3+} has the best photocatalytic activity. This indicated that the Fe^{3+} doped amount was very important to photoactivity of prepared TiO_2. That is, high or low doping level also decreases the photocatalytic activity of nanometer TiO_2 as shown in Fig. 8. A similar photocatalytic activity trend was also obtained for XRG and RhB dye degradation when Fe^{3+} was doped on TiO_2[23,24]. The increase in photocatalyic degradation efficiency with increase in the amount of Fe^{3+} is explained by the ability of the dopant Fe ion to act as a charge carrier trap site for e-.[25] But if Fe^{3+} content is excessive, the recombination rate increases exponentially with the doped concentration because the average distance between the trap sites decreases with increasing the number of dopants within a particle, thus reducing the quantum efficiency and the catalytic activity finally[26].

However, at high content of 25% and 50% in the Fe_2O_3/TiO_2 coupled oxides, the photocatalytic activity is less efficient than Degussa P25. Although the samples of 25% and 50% Fe_2O_3/TiO_2 increase greatly the absorption in whole range 350–500 nm (Fig.7), the weaker photocatalytic activity of the samples could be ascribed to the absorbed light majority consume away owing to the charge transfer transition between interacting iron ions and the d–d transition of Fe^{3+} causing the samples brown.

In addition to increase the photocatalytic degradation efficiencies under the UV light, the dopant Fe^{3+} ion also can significant shift the absorption edge towards the visible light, and can increase the absorption of Fe^{3+}/TiO_2 in whole range 350–500 nm. Thus the photocatalytic activity of 0.05%Fe/TiO_2, 50%Fe/TiO_2, pure TiO_2 and Degussa P25 TiO_2 were also comparably carried out under irradiation of sunlight and the results are shown in the Fig. 9. From the figure, we can find that the photocatalytic activity of prepared pure TiO_2 and 0.05%Fe/TiO_2 even exceeds that of Degussa P25 under sunlight, The highly phtotcatalytic activity of the samples is due to the probably factors that the samples prepared by the precursor of TiO_2 added surfactants and dried with ultrasonic method possess relative large surface area, good anatase crystallinity, small crystallite size and pore volume, resulting in a good photocatalytic activity[26, 27].

Fig. 10 also showed the photocatalytic degradation profiles of TiO_2 doped with different kind anions Fe^{3+} salt. It is obvious that the degradation efficiency of MO displays a decreasing order as follows: $Fe_2(SO_4)_3/TiO_2$ > $FeCl_3/TiO_2$ > $Fe(NO_3)_3/TiO_2$ > FC/TiO_2. As we know, Cl^-, NO_3^-, SO_4^{2-} has larger ionic radius than O^{2-}, so they cannot substitute O^{2-} in TiO_2 lattice and must be absorbed on the titania surface[28]. After calcinations, these inorganic anions were absorbed onto the surface of TiO_2, while the citrate anion was completely removed by burning. Therefore, a little SO_4^{2-} added TiO_2 generated some acidic sites on the surface of nanometer particles. Further more, these acidic sites were beneficial for the adsorption of organic compound molecules and for the inhibition of the recombination between photogenerated electrons and holes because of the captured effect of these acidic sites for photo-induced electrons[29]. Moreover, the highly polarized state of surface acidity would be profitable for the trapping of electrons on the UV-excited TiO_2, resulting in an improved quantum yield with producing reactive hydroxyl group radicals[30]. While the electron negativity of Cl^- and NO_3^- ions is weaker than SO_4^{2-}, the quantum yield with generating reactive hydroxyl group radicals would be lower.

Conclusion

The highly phtotcatalytic activity nanometer iron doped TiO_2 particles were prepared by a simple and traditional synthetic route with ultrasonic. Over 1% Fe content doped TiO_2 powders showed a strong absorption in whole range 350–500 nm and a red shift in the band gap but showed the weaker photocatalytic activity under UV and sunlight owing to the brown powders. A small amount of 0.05% Fe-doping could improve the photocatalytic activity of TiO_2 powders both under the UV light and sunlight, and the photocatlytic activity even higher than that of Degussa P25 TiO_2.

Acknowledgement

This work was financially supported by the National Nature Science Foundation of China (No. 40572173), the Science and Technology Project of Guangdong Province China (No. 2006A36701002 and 2005A30401001) and Foshan City Science Foundation Grant (02060031).

References

1. Sumita T.S.,Yamaki T.T.Y. and Yamamoto S.Y., Photo-induced surface charge separation of highly oriented TiO_2 anatase and rutile thin films, *Applied Surface Science*, **200**, 21-26 (**2002**)

2. Hoffmann M.R., Martin S.T. and Choi W., Environmental applications of semiconductor photocatalysis, *Chem. Rev.*, 69-96 (**1995**)

3. Fujishima A.R., Rao Tata N. and Donald Tryk. Titanium dioxide photocatalysis, *J. Photochem. Photobio. C: Photochem.* 1–21 (**2000**)

Table I
The dependence of particles mean size of TiO_2 on different Fe^{3+} content

Sample	pure TiO_2	0.05% Fe^{3+}/TiO_2	1% Fe^{3+}/TiO_2	25% Fe^{3+}/TiO_2	50% Fe^{3+}/TiO_2
Mean Size (nm)	42.1	21.3	21.1	16.3	14.2

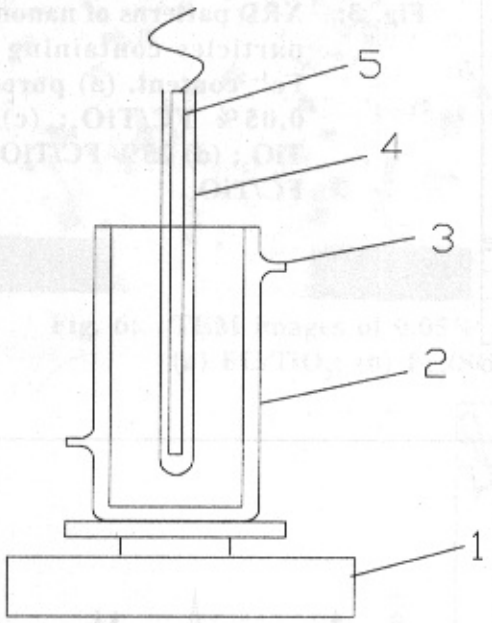

Fig. 1: Photocatalytic reactor. 1. Magnetic stirrer 2. Reactor 3. Cooling water 4. Quartz protection 5. UV lamp.

Table II
The dependence of particles mean size of TiO_2 on doping ferrous salt

Sample	FC*	$Fe(NO_3)_3$	$FeCl_3$	$Fe_2(SO_4)_3$
Mean Size(nm)	21.3	23.2	24.3	21.6

* denoted ferric citrate

4. Dvoranová D.N., Brezová V.L.S.T.,Mazúr M.L. et al., Investigations of metal-doped titanium dioxide photocatalysts, *Applied Catalysis B: Environmental*, **37**, 91–105 **(2002)**

5. Choi W, Termin A, Hoffmann M.R., The role of metal ions dopant in quantum-size TiO_2: Correlation between photoreactivity and charge carrier recombination dynamics, *J. Phys Chem*, **98**, 13669-13679 **(1994)**

6. Kang M., Synthesis of Fe/TiO_2 photocatalyst with nanometer size by solvothermal method and the effect of H_2O addition on structural stability and photodecomposition of methanol, *J. Mol. Catal A:Chem*, **197**, 173-183 **(2003)**

7. Zhang M.L., An T.C., Hu X.H. et al. Preparation and photocatalytic properties of a nanometer $ZnO-SnO_2$ coupled oxides, *Appl. Catal. A: General*, **260**, 215-222 **(2004)**

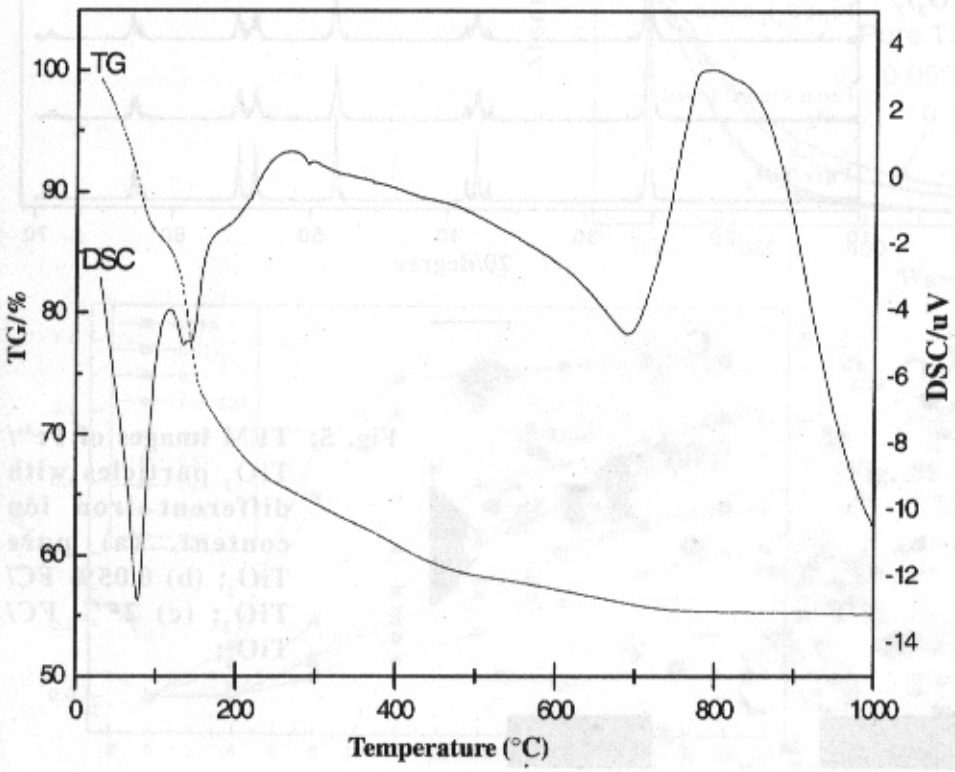

Fig. 2: Differential scanning calorimetry (DSC) and thermogravimetric (TG) analysis of nanometer TiO_2 precursor

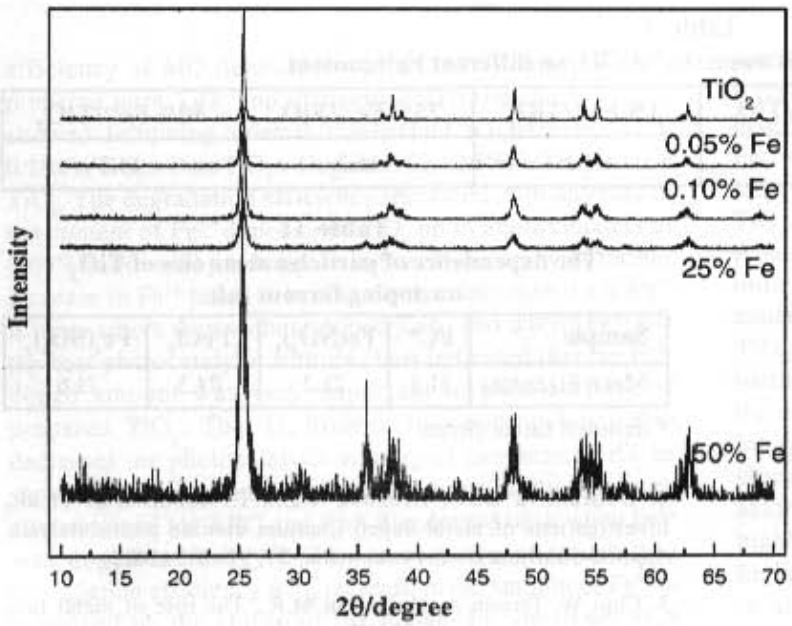

Fig. 3: XRD patterns of nanometer TiO_2 particles containing different Fe^{3+} content. (a) pure TiO_2; (b) 0.05% FC/TiO_2; (c) 1% FC/TiO_2; (d) 25% FC/TiO_2; (e) 50% FC/TiO_2.

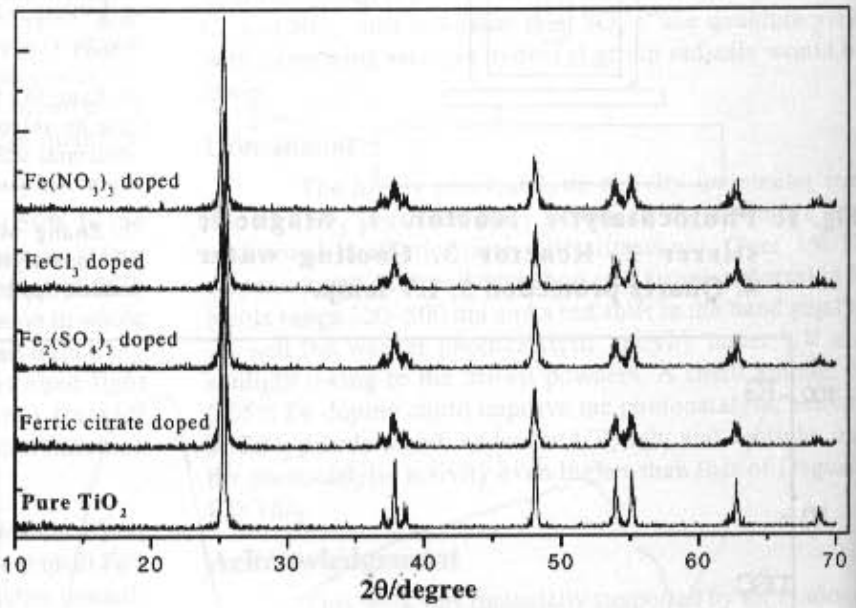

Fig. 4: XRD patterns of 0.05% Fe^{3+}/TiO_2 particles containing different anions. (a) pure TiO_2; (b) FC/TiO_2; (c) $Fe_2(SO_4)_3$/TiO_2; (d) $FeCl_3$/TiO_2; (e) $Fe(NO_3)_3$/TiO_2.

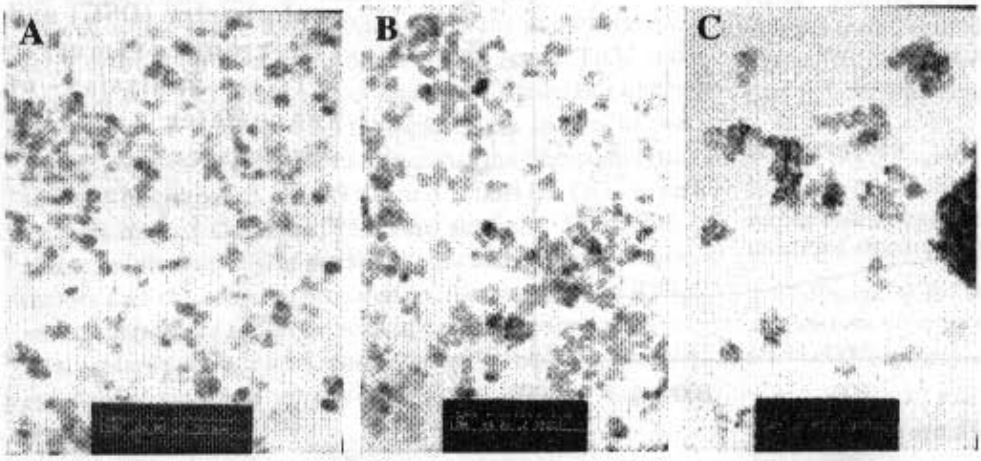

Fig. 5: TEM images of Fe^{3+}/TiO_2 particles with different iron ion content. (a) pure TiO_2; (b) 0.05% FC/TiO_2; (c) 25% FC/TiO_2;

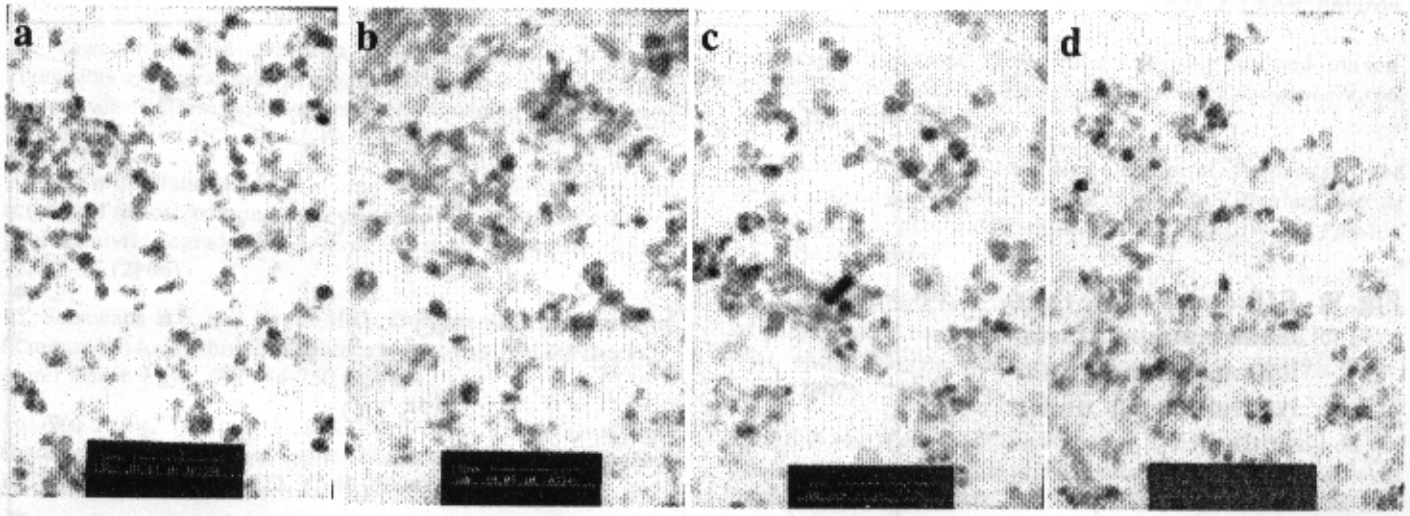

Fig. 6: TEM images of 0.05% Fe^{3+}/TiO_2 particles with different anions. (a) FC/TiO_2; (b) $Fe_2(SO_4)_3/TiO_2$; (c) $FeCl_3/TiO_2$; (d) $Fe(NO_3)_3/TiO_2$

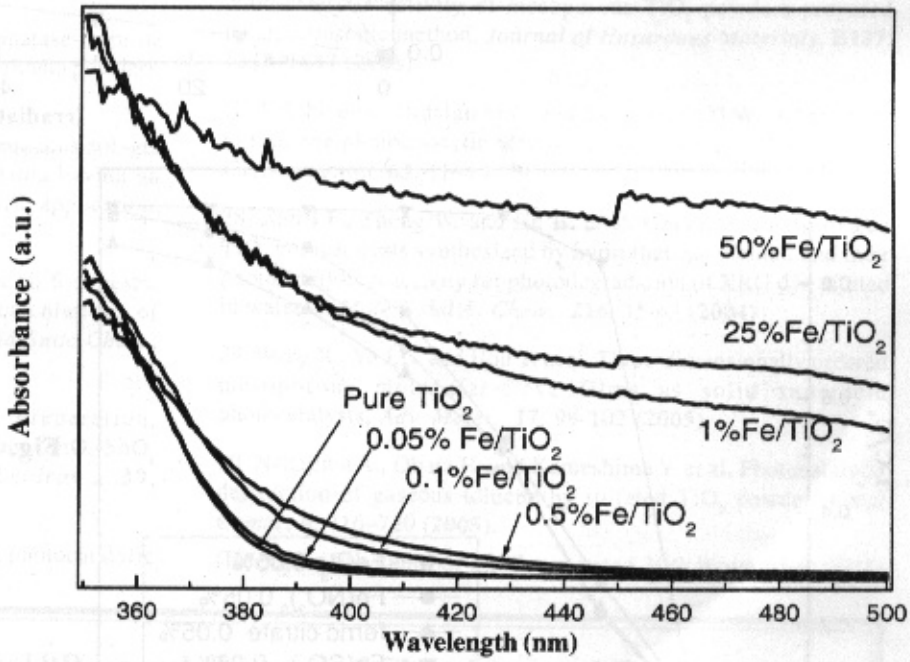

Fig. 7: UV-Vis diffuse reflectance spectra of prepared TiO_2 photocatalysts

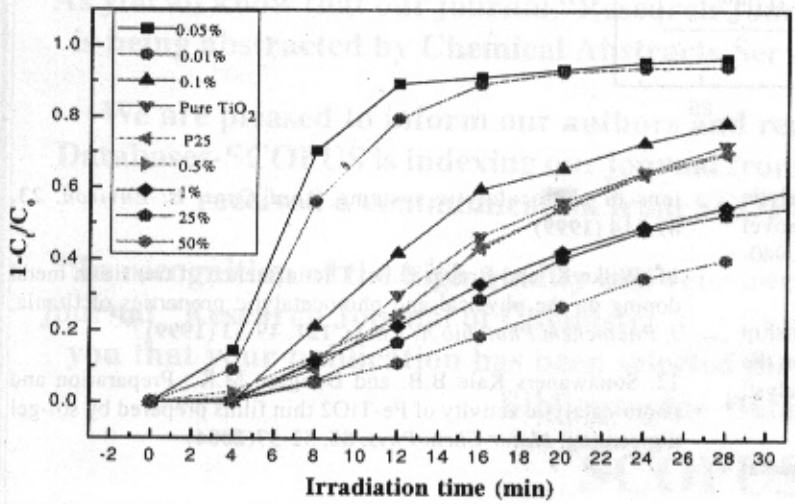

Fig. 8: Effect of different molar amount of iron ion on the photocatalytic efficiency under UV light

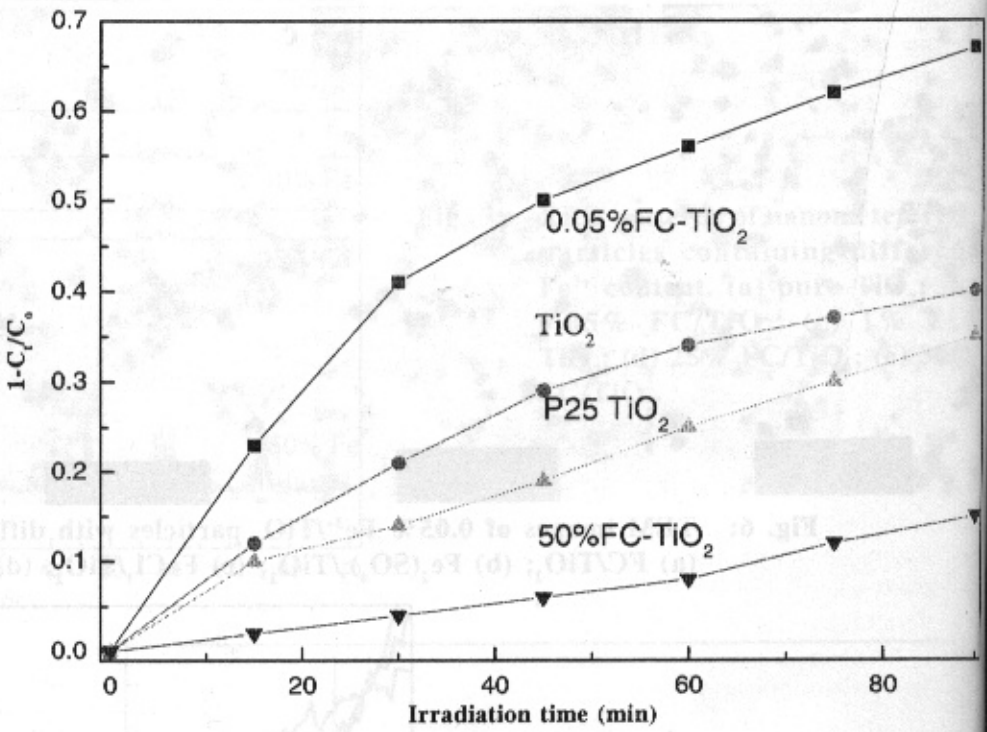

Fig. 9: Effect of different molar amount of iron ion on the photocatalytic efficiency under sunlight

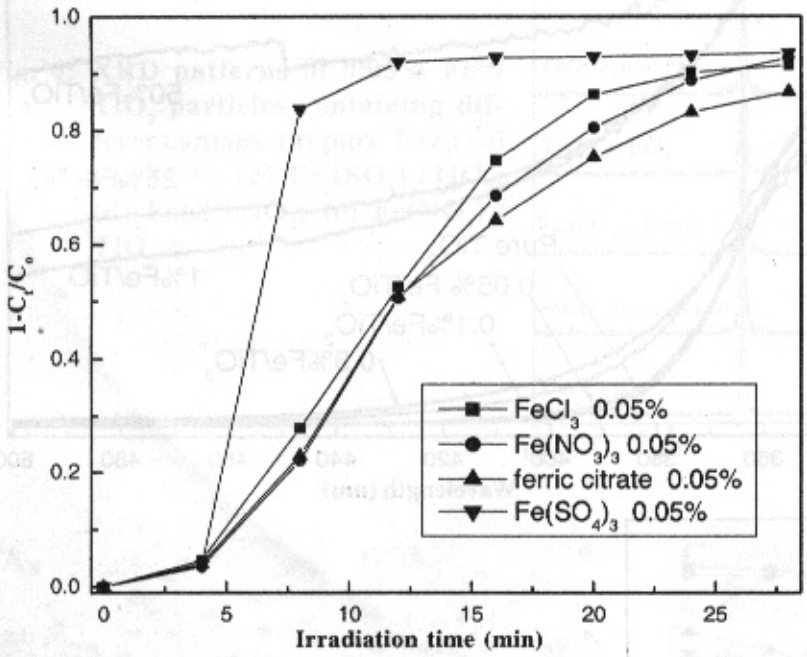

Fig. 10: Effect of different anions on th photocatalytic efficiency

8. Li J.L., Liu L. and Yu Y. et al. Preparation of highly photocatalytic active nano-size TiO_2 Cu_2O particle composites with a novel electrochemical method, *Electrochemistry Communications*, **6**, 940-943 (**2004**)

9. Piera E., Tejedor M.L. and Zorn M.E. et al, Relationship concerning the nature and concentration of Fe(III) species on the surface of TiO_2 particles and photocatalytic activity of the catalyst, *Appl Catal B: Environ*, **46**, 671-685 (**2003**)

10. Litter M.I., Heterogeneous photocatalysis: Transition metal ions in photocatalytic systems, *Appl Catal B: Environ*, 2 89-114 (**1999**)

11. Wilke K. and Breuer H.D., The influence of transition me doping on the physical and photocatalytic properties of titani *J. Photochem Photobio A: Chem*, **121**, 49-53 (**1999**)

12. Sonawaners Kale B.B. and Dongare M.K., Preparation a photo-catalytic activity of Fe-TiO2 thin films prepared by sol-g dip coating, *Mater Chem Phys*, **85**, 52-57(**2004**)

13. Yamashita H.M., Harada M.S.R., Misaka J.K. et al, Photocatalytic degradation of organic compounds diluted in water using visible light-responsive metal ion-implanted TiO_2 catalysts: Fe ion-implanted TiO_2, *Catalysis Today*, **84**, 191-196 (**2003**)

14. Ada´n C., Bahamonde A., Ferna´ndez A. et al, Structure and activity of nanosized iron-doped anatase TiO_2 catalysts for phenol photocatalytic degradation, *Applied Catalysis B: Environmental*, **72**, 11–17 (**2006**)

15. Sonawane R.S. and Hegde H.G., Dongaremk, Preparation of titanium(IV) oxide thin film photocatalyst by sol-gel dip coating, *Mater Chem. Phys.*, **77**, 744-750 (**2004**)

16. Wu X.D., Wang D.P. and Yang S.G., Preparation and characterization of stearate-capped titanium dioxide nanoparticles, *J. Colloid Interface Sci*, **222**, 37-40 (**2000**)

17. Sankapal B. R., Lux-Steiner M.C.H., Ennaoui A., Synthesis and characterization of anatase-TiO_2 thin films, *Applied Surface Science*, **239**, 165–170 (**2005**)

18. Ding X.Z. and Liu X.H., Correlation between anatase-to-rutile transformation and grain growth in nanocrystalline titania powders, *J. Mater Res.*, **13**, 2556-2559 (**1998**)

19. Baiju K., Sibu C.P. and Rajesh K. et al, An aqueous sol–gel route to synthesize nanosized lanthana doped titania having an increased anatase phase stability for photocatalytic application, *Mater Chem Phys*, **90**, 123–127 (**2005**)

20. Huang F.Q., Somers R.C., McFarland A.D. et al, Syntheses, structures, optical properties, and theoretical calculations of $Cs_2Bi_2ZnS_5$, $Cs_2Bi_2CdS_5$, and $Cs_2Bi_2MnS_5$, *J. Solid State Chem.*, **174**, 334-341 (**2003**)

21. Wang C., Zhao J.C., Wang X.M. et al, Preparation, characterization and photocatalytic activity of nano-ZnO_2-SnO_2 coupled photocatalyst, *Appl Catal B: Environ.*, **39**, 843–848 (**2002**)

22. Hung W.C., Fu S.H., Tseng J.J. et al, Study on photocatalytic degradation of gaseous, dichloromethane using pure and iron ion-doped TiO_2 prepared by the sol–gel method, *Chemosphere*, **66**, 2142–2151 (**2007**)

23. Zhou M.H., Yu J.G. and Bei C.G., et al, Preparation and photocatalytic activity of Fe-doped mesoporous titanium dioxide nanocrystalline photocatalysts, *Materials Chemistry and Physics*, **93**, 159–163 (**2005**)

24. Xin B.F., Ren Z.H.Y., Wang P. et al. Study on the mechanisms of photoinduced carriers separation and recombination for Fe^{3+}–TiO_2 photocatalysts, *Applied Surface Science*, **253(9)**, 4390-4395 (**2007**)

25. Qi X.H., Wang Zh.H. and Zhuang Y.Y. et al, Study on the photocatalysis performance and degradation kinetics of X-3B over modified titanium dioxide, *Journal of Hazardous Materials*, **B118**, 219–225 (**2005**)

26. Zhou M.H., Yu J.G. and Cheng B., Effects of Fe-doping on the photocatalytic activity of mesoporous TiO_2 powders prepared by an ultrasonic method, *Journal of Hazardous Materials*, **B137**, 1838–1847 (**2006**)

27. Sakthivel S., Hidalgo M.C. and Bahnemann D.W., A fine route to tune the photocatalytic activity of TiO_2, *Applied Catalysis B: Environmental*, **63**, 31–40 (**2006**)

28. Zhu J.F., Zheng W. and He B. et al, Characterization of Fe–TiO_2 hotocatalysts synthesized by hydrothermal method and their photocatalytic reactivity for photodegradation of XRG dye diluted in water, *J. Mole Catal A: Chem.*, **216**, 35-43 (**2004**)

29. Wang X., Yu J.C. and Hou Y. et al. Three-dimensionally ordered mesoporous molecular-sieve films as solid superacid photocatalysts, *Adv. Mater*, **17**, 99-102 (**2005**)

30. Nakajima A., Obata H. and Kameshima Y. et al, Photocatalytic destruction of gaseous toluene by sulfated TiO_2 powder, *Catal Comm.*, **6**, 716–720 (**2005**).

(Received 5th October 2007, accepted 30th November 2007)